

NO_x Abatement using DBD Nonthermal Plasma: Effect of Reactor Configurations

Luigi Amato

Dipartimento di Ingegneria Chimica,
Materiali e della Produzione
Industriale;
Università degli studi di Napoli
"Federico II";
Napoli, Italy; ;
luigi.amato2@unina.it

Maysam Abbod

Department of Electronic and
Computer Engineering;
Collage of Engineering,
Design and Physical Sciences;
Brunel University;
Uxbridge, London, United Kingdom

Nadarajah Manivannan

Department Design;
Collage of Engineering,
Design and Physical Sciences;
Brunel University;
Uxbridge, London, United Kingdom.

Francesco Di Natale

Dipartimento di Ingegneria Chimica,
Materiali e della Produzione
Industriale;
Università degli studi di Napoli
"Federico II";
Napoli, Italy.

Amedeo Lancia

Dipartimento di Ingegneria Chimica,
Materiali e della Produzione
Industriale;
Università degli studi di Napoli
"Federico II";
Napoli, Italy.

Wamadeva Balachandran

Department of Electronic and
Computer Engineering;
Collage of Engineering,
Design and Physical Sciences;
Brunel University;
Uxbridge, London, United Kingdom.

Abstract—This paper reports the results of NO reduction to N₂ and O₂ using two different DBD reactors with cylindrical configurations: a coaxial reactor with two dielectric barriers and a single dielectric barrier. The capability of the non-thermal plasma to convert NO to N₂ and O₂ was evaluated starting from a model flue gas at the compositions of 80-500 ppm of NO in N₂. The applied voltage, frequency and the NO flow rate were investigated to measure their effects in terms of the NO_x reduction efficiency. A screw thread was used as high voltage electrode in the one dielectric barrier configuration to establish a higher electric field strength in the gas gap and hence higher electron density. An increasing electron density improve the nitrogen electrical dissociation that encourage the NO_x conversion. This configuration was more suitable for the intended application. Indeed, almost the totality of the NO was converted to N₂ and O₂ with the two dielectric barriers configuration at the maximum NO mass flow rate of 50 mg_{NO}/h; while the same conversion was achieved using one dielectric barrier configuration at the maximum NO mass flow rate of 200 mg_{NO}/h. The higher the gas flow rate can be treated by fixing the desired conversion, the higher is the industrial interest in this process.

Keywords—NO_x, atmospheric-pressure plasmas, non-thermal plasma, nitrogen plasma, dielectric barrier discharge, Discharges (electric).

I. INTRODUCTION

One of the main worldwide challenge in the 21st century is the emission control for the environmental protection. NO_x represents one of the most important gaseous pollutants due to its role in the formation of fine particles, smog, acid rain and eutrophication. NO_x is mainly produced by combustion processes both from stationary sources (power plants, industrial combustion, domestic heating) and transportation. The most common de-NO_x technologies are the selective catalytic reduction (SCR) [1], [2] and the selective non-catalytic reduction (SNCR) [3], [4]. Both technologies use a reducing agent, like ammonia or urea, to convert NO_x into

harmless compounds either on the catalytic surface (in the SCR) or in the gas phase (in the SNCR). Even if the SCR is largely used due to its high efficiency, it has several drawbacks like the sulphur sensitivity, the high temperature required to activate the catalyst and the ammonia slip. An alternative strategy is the direct decomposition of NO_x to N₂ and O₂. This conversion is not spontaneous and it requires the presence of a catalyst to occur [5], [6]. However, the presence of oxidising species in the carrier gas like O₂ or CO₂ drastically reduces the NO_x conversion efficiency.

In the last decades, non-thermal plasma (NTP) processes have been proposed for the NO_x conversion to N₂ and O₂ as an alternative to the direct decomposition. The NO_x conversion can achieve an efficiency of about 98% as the NTP is applied to a gas that does not contain oxygen or other oxidizing species [7], [8]. A two-stage process consisting of a NO_x adsorption stage followed by a NTP reduction stage have been also proposed for gas cleaning applications [9]–[12]. During the adsorption, NO_x is trapped on the sorbent surface, purifying the gas current. During the sorbent regeneration, N₂ desorbs the NO_x adsorbed, restoring the adsorption capacity of the sorbent. The current made of NO_x concentrated in N₂ can be treated in an NTP reactor to reduce NO_x to N₂ and O₂.

The Dielectric Barrier Discharge (DBD) is one of the most commonly used electrical discharge to promote the non-thermal plasma generation at atmospheric pressure [13], [14]. The presence of dielectric limits the average current density in the gas space, it plays the role of distributed resistive load that prevents high currents and dielectric breakdown. The typical AC electric field strength needed to sustain non-thermal plasma is about 10⁶ V/m and the gas gap is often less than 1 cm.

In our previous study, a NO_x adsorption and NTP desorption with granular activated carbon (GAC) were proposed [15]. The desorption stage restored the sorbent

adsorption capacity and the NO_x desorbed was reduced to N₂ and O₂.

In the present study, two different DBD reactor configurations are proposed to determine the best reactor design to reduce NO_x coming from the desorption stage of the adsorption/NTP combined process. The NO_x conversion was investigated in a two dielectric barriers reactor and in a one dielectric barrier reactor. The first configuration allowed to preserve both the electrodes from the deterioration and encouraged a homogeneous electric field in the gas gap. The latter configuration used a screw thread as a High Voltage (HV) electrode to improve the local electric field and encourage the formation of electron avalanches.

II. EXPERIMENTAL SETUP AND METHODS

A. Experimental Setup

The experimental setup is showed in Figure 1. The model flue gas was produced starting from the N₂ and 1000 ppm of NO in N₂ gas cylinders. The flow rate and the concentration were adjusted by two digital flowmeters before the reactor. The gas analyzer “Testo 350” was used to measure the NO_x (NO and NO₂) concentration and temperature in continuous mode. The analyzer was placed at the exit of the reactor and operated with 1 L/min gas feed. A gas analyzer bypass was designed to collect the excess gas. The power generator section consists of a 20 MHz Function generator (TTi TG120), a high-voltage power amplifier (Trek Model 20/20C), a digital storage oscilloscope (Tektronix TBS1000B)

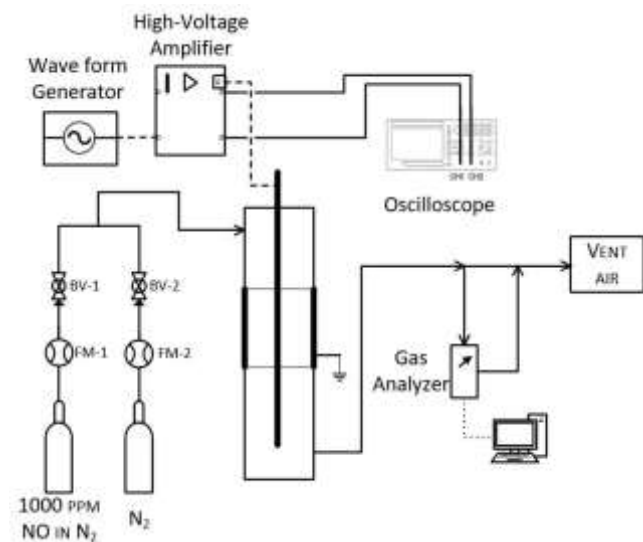


Figure 1 - Layout of experimental Setup.

B. DBD configurations

The model flue gas was prepared and it passed through the DBD reactor from the top to the bottom as shown in Figure 1. Two different reactors were tested and they are shown in Figure 2. The two dielectric barriers reactor comprised a steel rod electrode with a diameter of 5 mm, a quartz glass tube (inner diameter = 5 mm, outer diameter = 8 mm), a

borosilicate glass tube (inner diameter = 18 mm, outer diameter = 22 mm), a copper tape attached to the outer surface of the bigger glass tube. The one dielectric barrier reactor comprised a steel screw thread electrode of standard size M5, a borosilicate glass tube (inner diameter = 45 mm, outer diameter = 50 mm), a copper tape attached to the outer surface of the glass. The effective lengths of the ground electrodes were 30 cm for both the reactors.

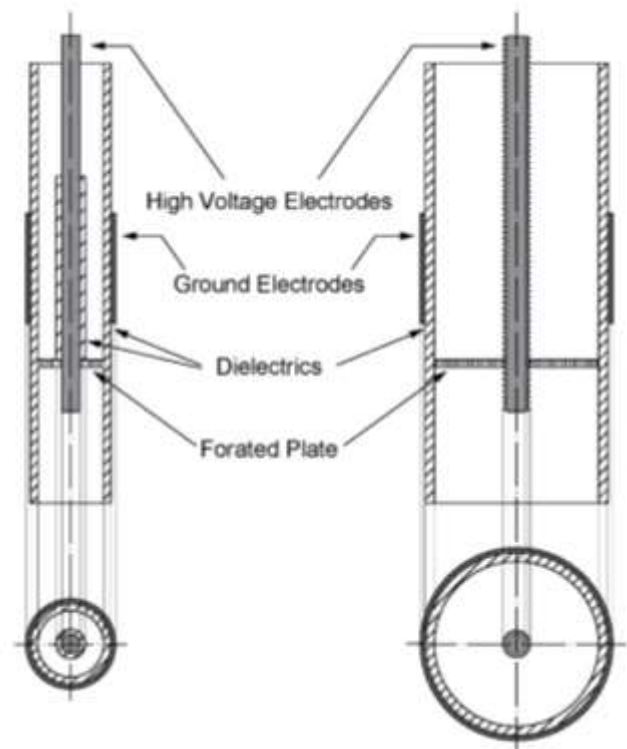


Figure 2 - Reactors configuration: two dielectrics barrier reactor of 22 mm (left), one dielectric barrier reactor of 50 mm (right).

C. Operating conditions

The experiments were performed at room temperature and at atmospheric pressure. The plasma was generated by applying a square wave potential of 38 – 40 kV pk/pk. The range of frequency investigated was 500 – 1000 Hz with a rise time of about 200 μs. The gas contained between 80 and 500 ppm of NO diluted in N₂ with a gas velocity of 0.1 – 1.2 m/s.

The NO mass flow parameter is introduced as a variable to study the NO conversion to N₂ and O₂. It is calculated from:

$$Q'_{NO} = c_{NO}^0 \cdot Q_{tot} \quad (1)$$

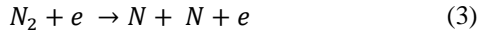
where c_{NO}^0 and Q_{tot} represent respectively the NO concentration and the total flow rate at the inlet. The NO conversion efficiency to N₂ and O₂ is calculated from the following equation:

$$NO \text{ conversion} = \frac{c_{NO}^0 - c_{NOx}^{out}}{c_{NO}^0} \cdot 100 \quad (2)$$

where c_{NOx}^{out} represents the NO_x concentration at the outlet of the reactor. NO_x has been considered as the sum of NO and

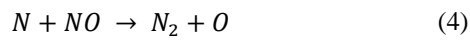
NO₂. In fact, many authors in the past demonstrated that NO diluted in N₂ mainly converts in N₂ and O₂ under the plasma condition. A small amount of NO can be converted into NO₂ [14], [16]. The gas composition of the tests performed in this study was mainly made of N₂ (almost 99%).

The electron impact dissociation of nitrogen occurs as the plasma is generated in an almost pure N₂ gas:

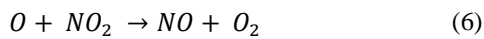
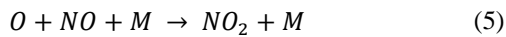


The description of the complex reaction path for this system is beyond the scope of this work and can be found, for example in [17]. However, a simplified description of the NO and NO₂ reduction can be summarised as follows.

The dissociated nitrogen radicals mainly react with the NO molecules to reduce them by producing oxygen radicals:



The dominant reactions that involve the oxygen radicals produced are the following [18].



Where M represents the third body reaction species.

III. RESULTS AND DISCUSSIONS

A. Two dielectric barriers discharge reactor

The capability to reduce NO to N₂ and O₂ depends on many variables: the NO concentration, the gas flow rate, the voltage applied and the frequency. When the plasma occurs, on almost pure nitrogen gas, the dissociation of molecules takes place. The nitrogen radicals produced from the dissociation react with the other molecules like NO to convert them into N₂ and O₂ e.g. Hence, the NO_x molecules' concentration decreases as the effect of their conversion to other species. Figure 3 shows the NO, NO₂ and NO_x concentrations as a function of time when 38 kV pk/pk was applied at the frequency of 1 kHz to the HV electrode in the two dielectric barriers configuration. The experimental results showed in Figure 3 were obtained by feeding 500 ppm of NO in N₂.

NO concentration exponentially decreased and achieved a 97% reduction after one minute. Then, the NO concentration decreased further down to 5 ppm after three minutes that correspond to a conversion of 99%. The NO₂ concentration remained low as almost the totality of NO were converted to N₂ and O₂. In fact, the reaction rate of (3) and (4) is much higher than (5) [16].

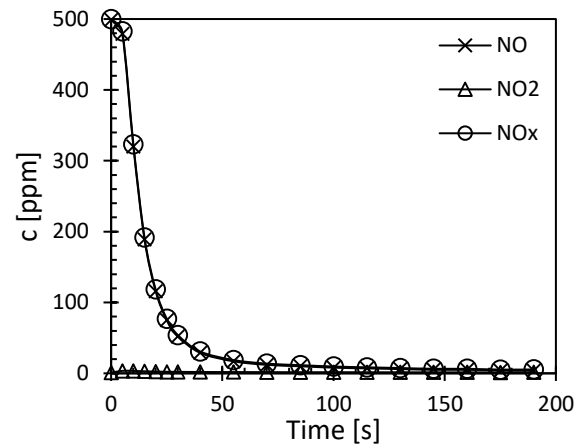


Figure 3 - NO, NO₂, NO_x emissions at 38 kV pk/pk and 1 kHz for the configuration with two dielectrics.

Figure 4 shows the dependence of the NO conversion as a function of the gas flow rate and at different NO inlet concentrations. The plasma was produced by applying 38 kV pk/pk at the frequency of 1 kHz.

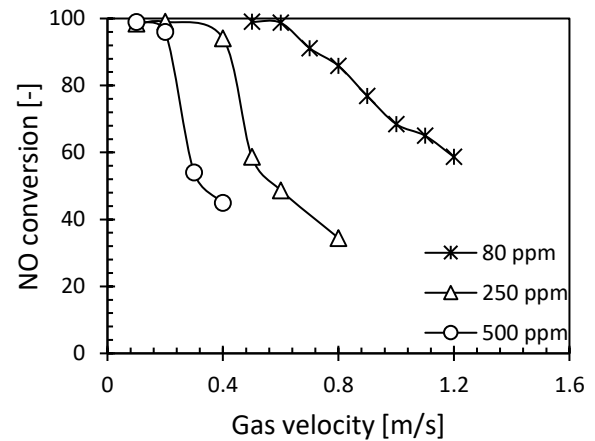


Figure 4 - Gas composition influence on the NO conversion for the configuration with two dielectrics at 38 kV and 1 kHz.

The NO conversion into N₂ and O₂ decreased as the gas velocity increased. The number of NO molecules passing through the plasma region in a unit of the time increased while, the energy required to convert NO per unit of molecules remained constant [7].

The NO conversion efficiency depends on the applied electric field promoting the generation of plasma in the DBD reactor. The higher the applied potential and frequency, the higher the NO conversion. Figure 5 and Figure 6 show the NO conversion efficiency as a function of the applied voltage and the frequency respectively. The results shown in Figure 5 were obtained at 80 ppm of NO in N₂ by applying 38 and 40 kV pk/pk at the fixed frequency of 1000Hz. The results shown in Figure 6 were obtained at 80 ppm of NO in N₂ by applying 38 kV pk/pk. The frequency was changed from 500 Hz to 1000Hz.

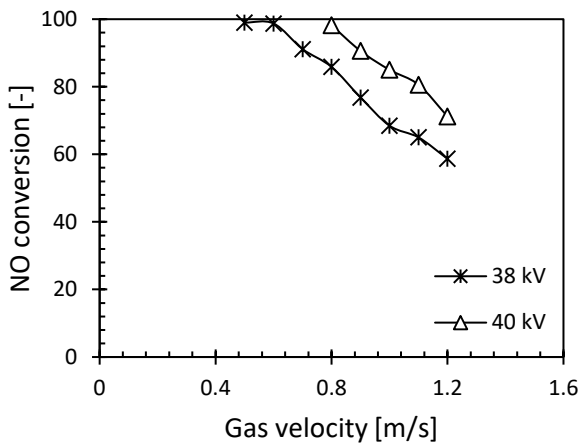


Figure 5 - Applied voltage dependence of NO conversion efficiency for the configuration with two dielectric barriers at 1 kHz.

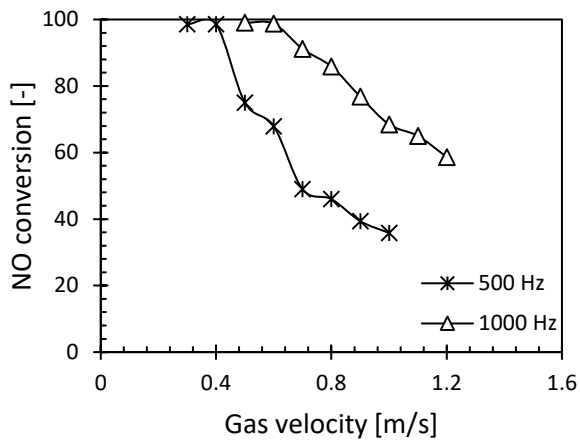


Figure 6 - Frequency dependence of NO conversion efficiency for the configuration with two dielectric barriers at 38 kV pk/pk.

The higher the applied potential and frequency, the higher the power supplied and the light intensity of the plasma [8]. The nitrogen dissociation is encouraged by the high electrical power supplied due to the abundance of free electrons in the gas gap. The higher number of nitrogen radicals produced from the dissociation encourages the NO conversion to N_2 and O_2 .

B. Configuration comparison

The plasma generated in the two dielectric barrier reactors appeared to be extremely thin streamers in the gas gap. The streamers spread all along the length of the electrode and were homogeneously distributed. The larger the reactor diameter, the lower the electric field in the gas gap.

The screw thread electrode used in the one dielectric barrier reactor was designed to improve the electric field. The sharp edges of the screw thread electrode produced a localized high-intensity electric field, which is similar to the tip of a needle that encourages the plasma production. The localized high-intensity electric field near the sharp edges increases the electron energy and produces a high number of secondary

electrons that develops to promote electron avalanche before it develops into streamers.

The plasma generated in the one dielectric barrier reactor configuration appeared as a series of pulsed streamers that started from the HV electrode and travelled toward the glass inner surface (dielectric barrier). The streamers branched out radially from the sharp edges and they were more scattered. These streamers were thicker for the one dielectric barrier reactor configuration than in the two dielectric barriers reactor. The presence of ramified streamers promoted a higher NO conversion due to the high plasma volume generated. However, the plasma volume did not correspond to the totality of the gas volume as in the two dielectric barriers reactor configuration. This is thought to be due to less homogeneous plasma generation.

The NO conversion is a function of the gas velocity and its concentration as shown in Figure 4. These NO conversion functionalities can be studied by defining the NO mass flow parameter as in (1). The curves showed in Figure 4 can be summarized by using one curve as shown in Figure 7. Figure 7 shows the NO conversion efficiency as a function of the NO mass flow for the two configurations under scrutiny. The NO conversion efficiency was always higher for the one dielectric barrier reactor than the configuration with the two dielectric barriers, even though the plasma generated in the single dielectric barrier reactor configuration was not homogeneous in the gas volume between the electrodes. This result can be attributed to the higher diameter of the one dielectric barrier reactor that allows a lower gas velocity by maintaining the same NO mass flow. The NO conversion efficiency remained constant at the value of 99% when the NO mass flow was lower than 200 mg_{NO}/h (for the one dielectric barrier configuration) that corresponds to about 80 ppm of NO and the flow rate of about 28 NL/min e.g. The efficiency decreased as the NO mass flow increased and it achieved the value of 50% when the mass flow was 700 mg_{NO}/h that corresponds to about 500 ppm and the flow rate of 18 NL/min e.g. The two dielectric barrier configurations could achieve the same efficiency only under a lower NO mass flow. The efficiency was 99% as the NO mass flow was lower than 50 mg_{NO}/h ; while it achieved the efficiency of 50% as the NO mass flow was about 170 mg_{NO}/h .

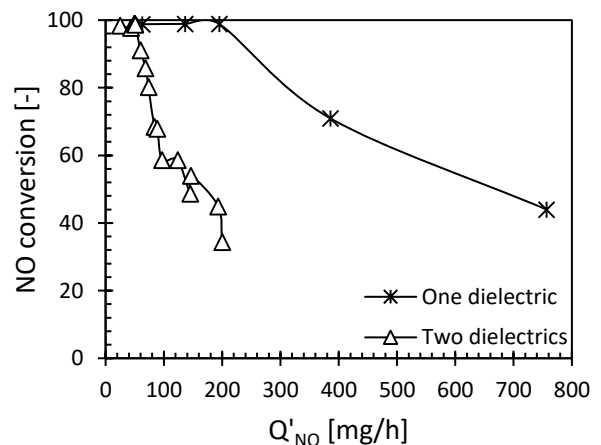


Figure 7 - NO conversion efficiency for the configurations: two dielectric barrier and one dielectric barrier reactors at 38 kV and 1kHz.

IV. CONCLUSIONS

We have conducted experiments on two different DBD configurations: two dielectric barrier reactor of 22 mm, one dielectric barrier reactor of 50 mm. The two dielectric barriers configuration allowed to generate a homogeneous plasma in the gas gap, making whole the gas passing through the plasma volume. The one dielectric barrier reactor used a screw thread as a high voltage electrode to encourage the plasma generation and to increase the plasma intensity even if the plasma volume did not involve all the gas volume between the electrodes. Both the configurations showed similar results in terms of NO conversion to N₂ and O₂, as a function of external parameters like gas flow rate, gas concentration, applied potential and frequency. The experiments showed that it is possible to convert NO to N₂ and O₂ with an efficiency of 99%. NO Removal efficiency decreased as the NO concentration in the inlet gas and the gas flow rate increased. The removal efficiency increased about 15-20% when the applied potential increased from 38 kV to 40 kV pk/pk. Likewise, the conversion efficiency increased by 50-80% when the frequency of the applied potential was increased from 500 to 1000 Hz.

A comparison between the two geometries was made in terms of NO removal efficiency as a function of the NO mass flow, which include both the flow rate and the concentration effects. The results showed that, in spite of the larger gas gap, the NO removal efficiency was always higher for the geometry having one dielectric barrier and the screw thread as a high voltage electrode. In particular, the efficiency of 99% was achieved as the NO mass flow increased up to 50 mg_{NO}/h, using the configuration with two dielectric barriers, and up to 200 mg_{NO}/h using the configuration with one dielectric barrier.

REFERENCES

- [1] B. Guan, R. Zhan, H. Lin, and Z. Huang, "Review of state of the art technologies of selective catalytic reduction of NO_x from diesel engine exhaust," *Appl. Therm. Eng.*, vol. 66, no. 1–2, pp. 395–414, 2014.
- [2] S. Brandenberger, O. Kröcher, A. Tissler, and R. Althoff, *The state of the art in selective catalytic reduction of NO_x by ammonia using metal-exchanged zeolite catalysts*, vol. 50, no. 4, 2008.
- [3] N. Irfan and A. Farooq, "Two-Stage NO_x Removal Using High Temperature Urea SNCR and Low Temperature Secondary Additive Injection," no. x, pp. 101–106.
- [4] U. Speer and A. Keiser, "High efficiency SNCR control system with online - CFD and NO_x prediction for the cement industry," *Conf. Proc. - IEEE-IAS/PCA Cem. Ind. Tech. Conf.*, vol. 2017-May, pp. 1–8, 2017.
- [5] N. Imanaka and T. Masui, "Advances in direct NO_x decomposition catalysts," *Appl. Catal. A Gen.*, vol. 431–432, pp. 1–8, 2012.
- [6] F. Garin, "Mechanism of NO_x decomposition," *Appl. Catal. A Gen.*, vol. 222, no. 1–2, pp. 183–219, 2001.
- [7] A. Mihalciou, K. Yoshida, M. Okubo, T. Kuroki, and T. Yamamoto, "Design factors for NO_x reduction in nitrogen plasma," *IEEE Trans. Ind. Appl.*, vol. 46, no. 6, pp. 2151–2156, 2007.
- [8] Z. Liu, Y. Cai, J. Wang, C. Sun, and W. Han, "A study on coaxial type DBD decomposing NO/N₂ mixture gas by optical emission spectrum," *Proc. - 2012 5th Int. Conf. Intell. Comput. Technol. Autom. ICICTA 2012*, pp. 657–661, 2012.
- [9] K. Yoshida, M. Okubo, T. Kuroki, and T. Yamamoto, "NO_x aftertreatment using thermal desorption and nitrogen nonthermal plasma reduction," *IEEE Trans. Ind. Appl.*, vol. 44, no. 5, pp. 1403–1409, 2008.
- [10] Q. Yu, H. Wang, T. Liu, L. Xiao, X. Jiang, and X. Zheng, "High-efficiency removal of NO_x using a combined adsorption-discharge plasma catalytic process," *Environ. Sci. Technol.*, vol. 46, no. 4, pp. 2337–2344, 2012.
- [11] X. Tang, F. Gao, J. Wang, H. Yi, and S. Zhao, "Nitric oxide decomposition using atmospheric pressure dielectric barrier discharge reactor with different adsorbents," *RSC Adv.*, vol. 4, no. 102, pp. 58417–58425, 2014.
- [12] T. Kuwahara, H. Nakaguchi, T. Kuroki, and M. Okubo, "Continuous reduction of cyclic adsorbed and desorbed NO_x in diesel emission using nonthermal plasma," *J. Hazard. Mater.*, vol. 308, no. x, pp. 216–224, 2016.
- [13] U. Kogelschatz, "Dielectric-barrier Discharges: Their History, Discharge Physics, and Industrial Applications," *Plasma Chem. Plasma Process.*, vol. 23, no. 1, pp. 1–46, 2003.
- [14] A.-M. Zhu, Q. Sun, J.-H. Niu, Y. Xu, and Z.-M. Song, "Conversion of NO in NO/N₂, NO/O₂/N₂, NO/C₂H₄/N₂ and NO/C₂H₄/O₂/N₂ Systems by Dielectric Barrier Discharge Plasmas," *Plasma Chem. Plasma Process.*, vol. 25, no. 4, pp. 371–386, Aug. 2005.
- [15] M. J. Luigi Amato, Naradajah Manivannan, Wamadeva Balachandran, Francesco Di Natale, Maysam Abbod, "DBD plasma for NO_x adsorption and desorption-reduction using GAC for the marine emissions control," *IEEE Ind. Appl. Soc. Annu. Meet.*, pp. 1–8, 2017.
- [16] B. M. Penetrante, M. C. Hsiao, B. T. Merritt, G. E. Vogtlin, and P. H. Wallman, "Comparison of Electrical Discharge Techniques for Nonthermal Plasma Processing of NO in N₂," *IEEE Trans. Plasma Sci.*, vol. 23, no. 4, pp. 679–687, 1995.
- [17] J. De Wilde, C. Lorant, and P. Descamps, "2D modeling and simulation of the flow dynamics, electric field and reactions in a low-temperature, atmospheric-pressure nitrogen plasma sharp-end plate-to-plane configuration and CVD reactor," *J. Phys. D: Appl. Phys.*, vol. 50, no. 13, 2017.
- [18] R. Atkinson, *Evaluated Kinetic and Photochemical Data for Atmospheric Chemistry Supplement IV IUPAC Subcommittee on Gas Kinetic Data Evaluation for Atmospheric Chemistry*, vol. 21, no. 6, 1992.

